Compact Multilayer Substrate Integrated Waveguide Dual-band Filtering Rat-race Coupler Based on Fan-shaped Cavities

Zhigang Zhang, Yong Fan, Yujian Cheng, and Yonghong Zhang

Fundamental Science on Extreme High Frequency Key Laboratory
University of Electronic Science and Technology of China, Chengdu 611731, China
freemanzzg@163.com, yfan@uestc.edu.cn, chengyujian@uestc.edu.cn, zhangyhh@uestc.edu.cn

Abstract ─ A new type of multilayer dual-band filtering rat-race coupler based on fan shaped substrate integrated waveguide (SIW) cavity is first proposed in this paper. Resonant frequencies of SIW fan-shaped cavity (SIFC) have been derived to construct a resonant cell. Magnetic and electric coupling between SIFCs are realized through multiple rectangular and circular slots located on metal layer, respectively. Specifically, the multiple rectangular slots are beneficial to increase coupling bandwidth and achieve better amplitude and phase balance. Moreover, the bandwidth ratio and center frequency of two pass-bands can be flexibly controlled by adjusting the size of band-stop resonators. The detailed analysis and the design method based on coupling matrix have been introduced to realize a dual-band filtering rat-race coupler. The new type of component should be able to provide at least three functions simultaneously, including in-phase and out-of-phase power dividing, filtering, and dual-band operation. Compared with other filtering couplers, the proposed design exhibits good dual-band filtering responses, high *Q* factor, better isolation, amplitude balance, as well as 0° and 180° phase differences.

Index Terms ─ Dual-band, filtering rat-race coupler, multilayer, substrate integrated fan-shaped cavity (SIFC).

I. INTRODUCTION

Rat-race couplers are essential components in transceivers for microwave communication systems, which can operate as an in-phase or out-of-phase power divider by properly choosing the excitation ports. As such, it can be used in the design of numerous components such as power amplifiers, balanced mixers, and antenna array feeding networks.

Meanwhile, the rapid development of various wireless communication systems has also led to the demand of dual-band operations in filters and couplers, which hold the promise for multichannel design. The emerging substrate integrated waveguide (SIW) technology [1-10] provides such a platform that can easily apply the dual-band or multilayer technology to the design of couplers and filters, and facilitate the miniaturization design of couplers and filters [11-12], which is becoming one of the primary trends for SIW components. In [1], synthesis and design techniques of dual-band filters are proposed. On one hand, the use of multilayered topologies [3-6] is known to provide more freedom to design coupling paths between waveguided structures while maintaining a compact circuit size [9]. A compact multilayer dual-mode filter based on the substrate integrated circular cavity (SICC) is developed in [6]. A design method for multiband bandpass filters with multilayer configuration is proposed in [10].

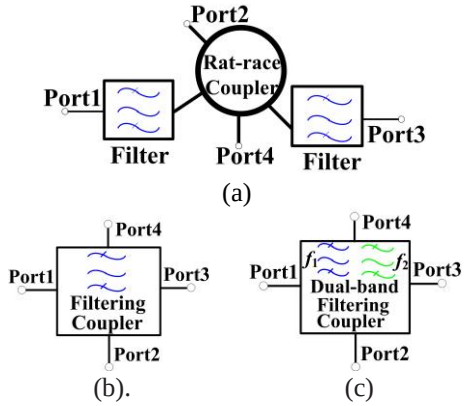

Fig. 1. (a) Cascaded filter and rat-race coupler, (b) single-band filtering rat-race coupler, and (c) dual-band filtering rat-race coupler.

Generally, couplers and filters are cascaded in transceivers front ends with the topology shown in Fig. 1 (a). Two filters are needed to integrate bandpass responses into a rat-race coupler, which leads to a large circuit area, a complex configuration and unwanted loss. On the other hand, to further reduce size, a single device integrated with different functionalities, such as filtering coupler [12-25], has been attracting increasing attention. It also recommends an effective way to avoid the performance degradation due to a cascade connection of two individual components, as shown in Fig. 1 (b).

Submitted On: February 13, 2020
Accepted On: February 28, 2020

Bandpass 90° and 180° directional couplers with coupled resonators have been first proposed in [13]. A compact filtering 180° hybrid is presented in [16]. Based on our knowledge, there are two methods [24-25] to realize the in-phase and out-of-phase operations in SIW rat-race coupler. Four TE_{101}-mode square cavities based on multilayer coupling structures are utilized to construct the filtering rat-race coupler [24]. A SIW filtering rat-race coupler based on TE_{102} and TE_{201} orthogonal degenerate modes is proposed in [25]. However, the above-mentioned filtering couplers can only operate in single frequency band. It is noteworthy that integrating dual-band technology into multifunctional components is a more effective way to realize miniaturization design. As shown in Fig. 1 (c), the dual-band filtering coupler is equivalent to cascading two single-band filtering couplers operating in different frequency band. The new type of component should be able to provide at least three functions simultaneously, including in-phase and out-of-phase power dividing, filtering, and dual-band operation. Moreover, the SIW filtering rat-race couplers with multiple frequency bands are rarely reported.

In this paper, a compact multilayer dual-band filtering rat-race coupler based on substrate integrated fan-shaped cavities (SIFCs) is proposed for the first time. The multilayer SIFC structure is not only compact, but also convenient for the realization of electric and magnetic coupling between resonators. Specifically, the magnetic coupling between SIFCs is obtained by using multiple rectangular slots, which increases the magnetic coupling strength and operation bandwidth, as well as achieves better amplitude and phase balance. Moreover, the bandwidth ratio and center frequency of two pass-bands can be flexibly controlled. What's unique about the analysis process of dual-band filtering rat-race coupler is that the bandwidth and center frequency of the corresponding broadband filtering coupler can be obtained from the specification of dual-band filtering coupler, due to the fact that the two passbands are formed by loading the bandstop resonator. The required coupling coefficient and external quality factor can be obtained by analyzing the topology of the single-band filtering coupler. Afterwards, the coupling matrix method is used to evaluate the initial value of design parameters accurately according to the specifications, which is beneficial to accelerate the later optimization design process. It's a good combination of multilayered topologies, multiband technology and multifunctional component, which realizes the miniaturization design of the coupler while keeping good performance.

II. ANALYSIS AND DESIGN

A. Coupler structure

As shown in Fig. 2, the multilayer SIW dual-band filtering coupler consists of fan-shaped SIW cavities coupled together by means of four rectangular slots and a circular slot etched in the common broad wall of adjacent SIFCs.

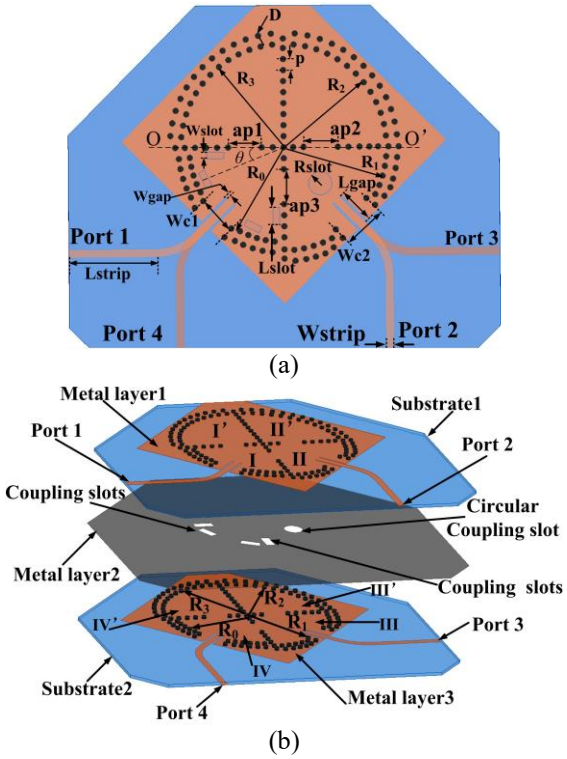

Fig. 2.The proposed multilayer SIFC dual-band filtering coupler: (a) top view and (b) anatomy view.

The configuration of the dual-band filtering coupler is illustrated in Fig. 2 (b).When signals are injected into port 1, the equal magnitude and phase signals are then taken out from port 2 and 4. However, when port 3 is excited, signals reach ports 2 and 4 through electrical and magnetic coupling, respectively. Then, the equal magnitude and opposite phase signals are acquired form port 2 and 4. Furthermore, two pairs TM_{101} SIFC bandstop resonators (Resonator I'~IV') are simultaneously coupling with TM_{101} SIFC bandpass resonators (Resonator I~IV) by the post-wall irises in the common post walls.

B. Analysis of coupler

The topology of the corresponding single-band filtering rat-race coupler is shown in Fig. 3 (a). As we can see, since each port of the coupler is loaded by a resonator, band-pass response can also be realized. Moreover, if each resonator (Resonator 1~4) is replaced by a dual-behavior unit (Unit1~4), a dual-band filtering rat-race coupler can be obtained.

Here, the dual-behavior unit is made up of two coupled resonators, as shown in Fig. 3 (b). Interestingly, the single-band filtering coupler could be regarded as a special case of dual-band filtering coupler by assuming $M11'=M22'=M33'=M44'=0$.

The topology of the dual-band filtering rat-race coupler is shown in Fig. 3 (b). As seen, the dual-band rat-race coupler has following two working states. When signals are injected from port 1, the output signals from ports 2 and 4 are in-phase, equal power allocation (M_{21}=M_{41}), just as an in-phase power divider should do. If port 3 is excited, the out-of-phase responses are obtained in ports 2 and 4 (-M_{23}=M_{43}). In this case, the coupler can be seen as an out-of-phase power divider. Moreover, the output signal has dual-band response characteristics.

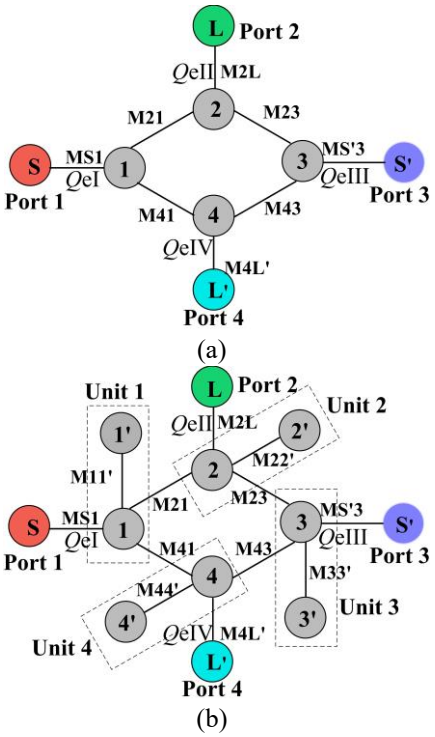

Fig. 3. (a) Topology of the corresponding single-band filtering coupler, (b) Topology of the multilayer dual-band filtering coupler, Unit1~4 represent dual-behavior resonator.

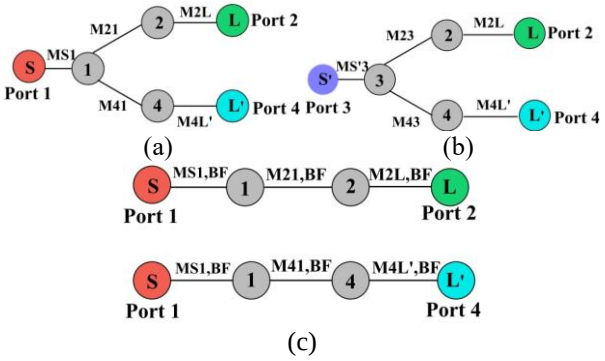

Fig. 4. (a) Topology of the filtering in-phase power divider, (b) topology of the filtering out-of-phase power divider, and (c) topology of two second-order filters.

As depicted in Figs. 4 (a) and (b), in these two working states, the single-band filtering coupler is equivalent to an in-phase filtering power divider and an out-of-phase filtering power divider, respectively. Moreover, divider I and II shown in Figs. 4 (a) and (b) are both designed with 3-dB power split ability and have same passband characteristics but quite different phase characteristic. Therefore, the coupling coefficients between resonators of dividers have the following relationship:

$$M_{21}=M_{41}=-M_{23}=M_{43}, \tag{1}$$

each power divider can be divided into two second-order bandpass filters which have the same operating frequency and passband characteristics, as shown in Fig. 4 (c). The coupling matrix of this second-order coupled-resonator band-pass filter is expressed as:

$$m_{N+2}=\begin{array}{c} \\ S \\ 1 \\ 2 \\ L \end{array}\begin{array}{c} \begin{array}{cccc} S & 1 & 2 & L \end{array} \\ \begin{bmatrix} 0 & m_{S1,BF} & 0 & 0 \\ m_{1S,BF} & 0 & m_{12,BF} & 0 \\ 0 & m_{21,BF} & 0 & m_{2L,BF} \\ 0 & 0 & m_{L2,BF} & 0 \end{bmatrix} \end{array}. \tag{2}$$

And the normalized input impedance of the filtering power divider in Fig. 4 (a) is required to be the same as matrix (2). Thus, the coupling coefficients for the filtering power divider topology in Fig. 4 (a) are determined as:

$$M_{S1,BF}=M_{S1}, \tag{3a}$$

$$M_{2L}=M_{4L'}=M_{2L,BF}=M_{4L',BF}. \tag{3b}$$

According to the filter design theory some elements in the matrix should be reduced by a factor of $\sqrt{2}$ to meet the requirement of input port matching of the power divider [18]:

$$M_{12}=M_{14}=\frac{M_{12,BF}}{\sqrt{2}}. \tag{4}$$

Based on (1), (2), and (4), the coupling matrix for the filtering power divider topology in Fig. 4 (a) is determined as:

$$M_{S1,BF}=M_{S1}, \tag{5a}$$

$$M_{2L}=M_{4L'}=M_{2L,BF}=M_{4L',BF}, \tag{5b}$$

$$M_{21}=M_{41}=-M_{23}=M_{43}=\frac{M_{21,BF}}{\sqrt{2}}=\frac{M_{41,BF}}{\sqrt{2}}. \tag{5c}$$

The required normalized coupling coefficient (m) and external quality factors (Q_e) for the filtering power divider can be calculated by:

$$m_{12}=\frac{M_{21}}{FBW}=\frac{M_{41}}{FBW},\quad m_{12,BF}=\frac{M_{21,BF}}{FBW}, \tag{6}$$

$$Q_e=\frac{FBW}{M_{S1}^2}=\frac{FBW}{M_{2L}^2}=\frac{1}{FBW\times m_{S1}^2}. \tag{7}$$

Generally, external quality factor (Qe) is related to the following two parameters: the length of feeding slot (Lgap), the width of external coupling aperture (Wc). In

order to obtain the same return loss and passband characteristics on each port, we have:

$$Q\text{eI}= Q\text{eII}= Q\text{eIII}= Q\text{eIV}=Q\text{e}. \quad (8)$$

C. Design considerations

Generally, the response of proposed dual-band filtering coupler with different bandwidth ratio can be divided into following three cases (Condition I~III).

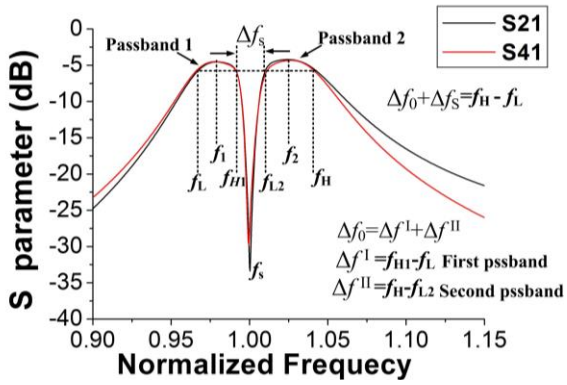

Fig. 5. Response of multilayer dual-band filtering coupler in Condition I ($\Delta f^{I}=\Delta f^{II}$, $f_s=f_0$).

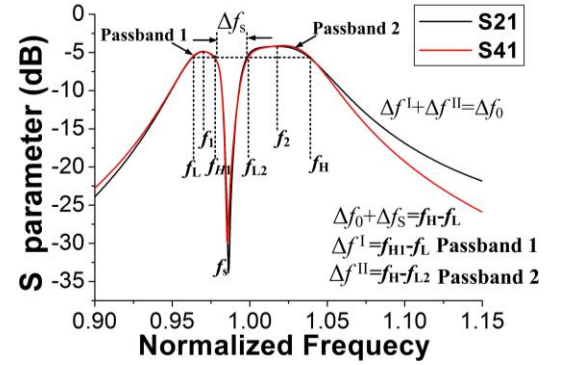

Fig. 6. Response of multilayer dual-band filtering coupler in Condition II ($\Delta f^{I}<\Delta f^{II}$, $f_s<f_0$).

In the first case, the bandwidth of two pass-bands is equal, and the bandwidth ratio equal to 1. Here, Δf^{I} and Δf^{II} represent absolute bandwidths (ABW) of passband 1 and passband 2, respectively. Figure 5 depicts response of the dual-band filtering coupler under Condition I. As seen, the dual-band filtering coupler creates two passbands (f_L, f_{H1}) and (f_{L2}, f_H). Where, f_1 and f_2 are the center frequencies of passband 1 and passband 2, respectively. f_0 and Δf_0 are the center frequency and bandwidth of the corresponding single-band filtering coupler. f_s and Δf_s are the center frequency and bandwidth of the stopband, respectively.

As shown in Fig. 6, the second case is that the bandwidth of the first passband is smaller than that of the second passband. In addition, the center frequency of stopband is less than that of the corresponding single-band filtering coupler.

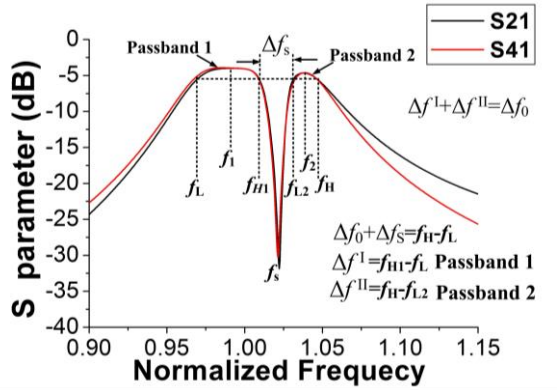

Fig. 7. Response of multilayer dual-band filtering coupler in Condition III ($\Delta f^{I}>\Delta f^{II}$, $f_s>f_0$).

Figure 7 plots the response of dual-band filtering coupler in Condition III, which demonstrates that the bandwidth of the passband 1 is larger than that of the passband 2. Due to the fact the two passbands are formed by splitting the frequency band of a broadband filtering coupler into two parts, combined with the topological structures, the bandwidth (BW) and center frequency of the corresponding single-band filtering coupler are obtained from the specification of the dual-band coupler ($f_0=\sqrt{f_L f_H}$, $\Delta f^{I}+\Delta f^{II}=\Delta f_0$), and the corresponding coupling coefficient and Qe can be obtained by analyzing the single-band filtering coupler, then the initial value of the internal coupling parameters and the length of the feeding slot can be determined.

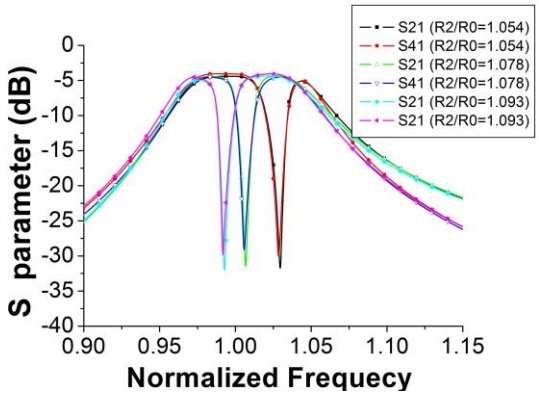

Fig. 8. Variation of stopband center frequency with R2/R0.

The central frequencies of dual-band filtering coupler are determined by the size of the band-pass

resonators (R0, R1). Besides, the radius of the band-stop resonators (R2, R3) is used to control the bandwidth ratio of the two pass-bands. As shown in Fig. 8, with the increase of R2/R0, the center frequency of the stopband decreases, thus the absolute bandwidths (ABW) of the pssband 1 and passband 2 can be adjusted. Throughout the entire procedure, it can be seen that the two passbands of this filtering coupler can be synthesized with prescribed BWs and center frequencies. The resonant frequency of mode for circular cavity with solid wall can be calculated by [34]:

$$f_{mpn}=\begin{cases}\dfrac{c}{2\pi\sqrt{\mu_r\varepsilon_r}}\sqrt{\left(\dfrac{\mu'_{mn}}{R}\right)^2+\left(\dfrac{p\pi}{\Delta h}\right)^2} & TE_{mpn}\\ \dfrac{c}{2\pi\sqrt{\mu_r\varepsilon_r}}\sqrt{\left(\dfrac{\mu_{mn}}{R}\right)^2+\left(\dfrac{p\pi}{\Delta h}\right)^2} & TM_{mpn}\end{cases},(9)$$

where μ_r and ε_r are relative permeability and permittivity of the filling material, μ_{mn} and μ'_{mn} are the nth roots of mth Bessel function of the first kind and its derivative, R is the radius of circular cavity, Δh is the height of the of circular cavity ,and c is the speed of light in free space. According to Equation 9 and by means of the least square method, the resonant frequency of the TM_{101} mode for SIFC can be calculated by the following formula:

$$f_{101}=\frac{0.383c}{\dfrac{1}{b_\theta}R_{eff}\sqrt{\mu_r\varepsilon_r}},\ R_{eff}=R-\frac{D^2}{0.95p}. \quad (10)$$

Where, θ is the central angle of SIFC, R_{eff} is the equivalent radius of the fan-shaped cavity. D and p are the diameter of metallized via-holes and center-to-center pitch between two adjacent via-holes. b_θ is related to the central angle of a fan-shaped resonator. When θ=60°, 90°, 120°, b_θ is approximately equal to 2.7, 2.1, 1.86, respectively.

D. Design example

In this design, the targeted specification of the dual-band filtering coupler is prescribed as follows:

1) Passband 1: 9.205–9.370 GHz (BW:165 MHz);
2) Passband 2: 9.565–9.875 GHz (BW:310 MHz);
3) In-band return loss: 20.0 dB.

According to the above analysis, the bandwidth and center frequency of the corresponding single-band filtering coupler are obtained from the specification of the dual-band coupler. The desired passband of single-band filtering coupler is centered at 9.535 GHz with the 2.9% fractional bandwidth (FBW) of 20-dB equal-ripple return loss (1-dB BW: 475MHz). Based on the advanced coupling matrix synthesis method in [33], the initial normalized coupling matrix of corresponding BPF can be synthesized as:

$$m_{N+2}=\begin{array}{c}\\S\\1\\2\\L\end{array}\begin{array}{c}\begin{array}{cccc}S & 1 & 2 & L\end{array}\\\begin{bmatrix}0 & 1.22474 & 0 & 0\\1.22474 & 0 & 1.65831 & 0\\0 & 1.65831 & 0 & 1.22474\\0 & 0 & 1.22474 & 0\end{bmatrix}\end{array}. \quad (11)$$

From (3)–(7), (11) the desired parameters of the filtering power dividers can be calculated as follows: M_{21}=M_{41}=-M_{23}=M_{43}=0.0343672, Qe,$_{S1}$=22.7465, Qe,$_{2L}$= Qe,$_{4L}$=22.7465. To extract Qe, full-wave simulations using ANSYS HFSS are carried out for the singly loaded SIFC excited by a 50-Ω microstrip line. The coupling strengths are controlled by the feeding slot length Lgap with fixed slot width Wgap = 0.3mm and coupling window width Wc = 5.35 mm. Qe can be extracted from the phase and the group delay response of S11 using [32]:

$$Qe=\frac{f_0}{\Delta f_{\pm 90^\circ}}. \quad (12)$$

Where, f_0 denotes the frequency at which the group delay of S11 reaches the maximum, $\Delta f_{\pm 90^\circ}$ indicates the ABW (absolute bandwidth) between ±90° points with respect to the absolute phase of S11 at f_0.

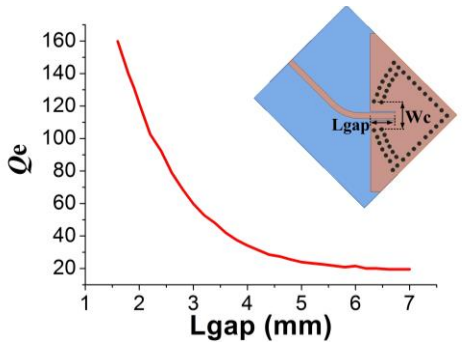

Fig. 9. Simulated external quality factor Qe change with Lgap, Wc=5.35mm.

Figure 9 shows the external quality factor Qe versus the length of feeding slot Lgap. It can be seen that the larger the feeding slots length, the smaller the external quality factor. The adjustment of external quality factor is realized by changing the value of Lgap, as depicted in Fig. 9. Then, the desired Qe (QeI = QeII = QeIII= QeIV= Qe) can be achieved and the initial value of Lgap can also be determined.

In general, the coupling coefficient of two coupled SIW cavities can be extracted by full-wave simulations. For two synchronously tuned coupled resonators, two split resonant frequencies can easily be identified by two resonance peaks, the coupling coefficient can then be evaluated using the formula [32]:

$$M_{ij} = \frac{f_{p2}^2 - f_{p1}^2}{f_{p2}^2 + f_{p1}^2}, \quad (13)$$

where f_{p1} and f_{p2} are the lower and higher resonant frequencies, respectively. Then, the relationship between coupling coefficients and physical structures of coupled resonators should be established.

The coupling coefficient M_{41} versus the rectangular slot length (Lslot) and offset angle (θ) are plotted in Figs. 10 (a) and (b). Obviously, when the lengths of the rectangular coupling slots increase, coupling coefficient also increases accordingly. In addition, the locations of coupling slots also have effect on the coupling strength between two SIW cavities.

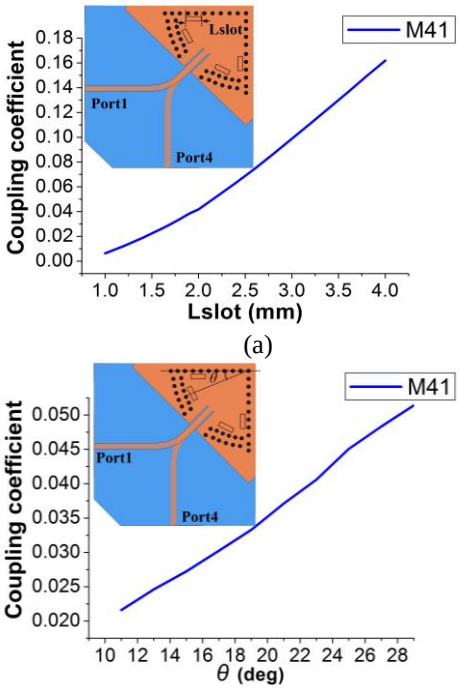

Fig. 10. Coupling coefficients versus the coupling slot: (a) M_{41} versus Lslot, Wslot=0.8mm, and (b) M_{41} versus θ, Lslot =1.85mm.

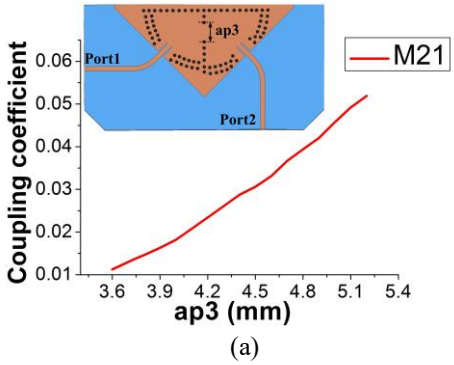

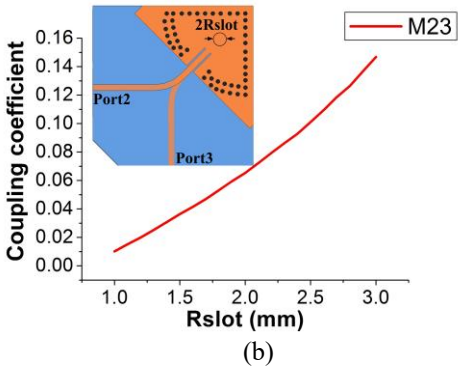

Fig. 11. Coupling coefficients versus the coupling slot: (a) M_{21} versus ap3 and (b) M_{23} versus Rslot.

Figure 11 illustrates the extracted curves of M_{21}, M_{23} which versus the width (ap3) and the radius (Rslot) of coupling slot, respectively.

In summary, the design procedure of the proposed dual-band filtering coupler is listed as follows. Firstly, the bandwidth (Δf_0) and center frequency (f_0) of the corresponding single-band filtering coupler are obtained from the specification of the dual-band filtering coupler. Then, the resonant frequency of the SIFC is calculated by formula (9) ~ (10), to meet the required center frequency f_0. Secondly, a coupling matrix of a second-order BPF is synthesized according to the desired center frequency f_0 and the fractional bandwidth (FBW). Thirdly, according to formulas (3) ~ (8), the coupling matrix and Qe of the corresponding filtering coupler are obtained. Moreover, internal coupling parameters (Lslot, θ, ap3, Rslot) and external coupling parameters (Wc1, Wc2, Lgap) are tuned to meet desired values of coupling coefficients and external quality factor, respectively. Finally, fine tuning of the entire structure is performed to realize good dual-band filtering rat-race coupler performance.

III. SIMULATED AND MEASURED RESULTS

After optimization implemented by HFSS, the geometry parameters of the proposed dual-band filtering coupler are chosen as follows (all in mm): R_0=12.9, R_1=14.15, R_2=R_3=14.2, ap3=4.77, Lgap=5.1, Wgap=0.3, θ=19deg, ap1=4.6 ap2=4.7, Rslot=1.4, Lslot=1.9, Wslot=0.9, Wc1=5.36, Wc2=5.96, Lstrip=11, Wstrip=1.15, D=0.8, p=1.5. To verify the above method, the proposed dual-band filtering coupler was designed and fabricated on a substrate with thickness of 0.508 mm, relative dielectric constant of 3.5 and dielectric loss tangent 0.0018 (at 10 GHz). The measurement is accomplished by using the Agilent N5244A network analyzer.

Figures 12 (a), (b) show the simulated and measured

S-parameters under the in-phase operation. The measured first passband is centered at 9.308 GHz with the 1-dB FBW of 1.62%. The in-band return loss is better than 15 dB. The minimum insertion losses including the 3-dB equal power division loss are (3+1.95) and (3+2.05) dB, with the amplitude imbalance of 0.1 dB.

The second passband is located at 9.738GHz with the 1-dB FBW of 3.12%. The in-band return loss is better than 18.5 dB. The minimum insertion losses including the 3-dB equal power division loss are (3+1.28) and (3+1.33) dB, with the amplitude imbalance of 0.1 dB.

Figures 13 (a), (b) show the simulated and measured S-parameters under the out-of-phase operation. The measured first passband is centered at 9.310GHz with the 1-dB FBW of 1.53%.The in-band return loss is better than 16 dB. The minimum insertion losses including the 3-dB equal power division loss are (3+1.99) and (3+2.08) dB, with the amplitude imbalance of 0.1 dB. The second passband are located at 9.739 GHz with the 1-dB FBW of 3.05%. The in-band return loss is better than 20 dB. The minimum insertion losses including the 3-dB equal power division loss are (3+1.35) and (3+1.4) dB, with the amplitude imbalance of 0.1 dB.

When signals are injected from port 1 and port 3, the measured in-band phase differences between two output ports are nearly 0° and 180°, respectively, with the variation of less than 3.5°, as depicted in Fig. 14.

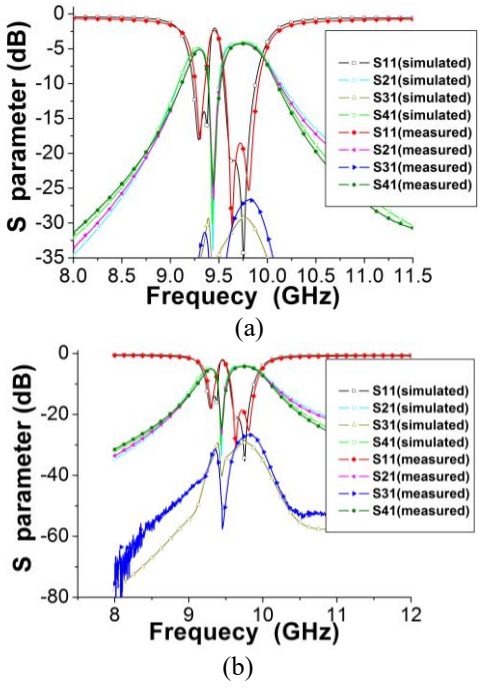

Fig. 12. Simulated and measured results of the fabricated dual-band filtering coupler: (a) and (b) Port 1 is excited.

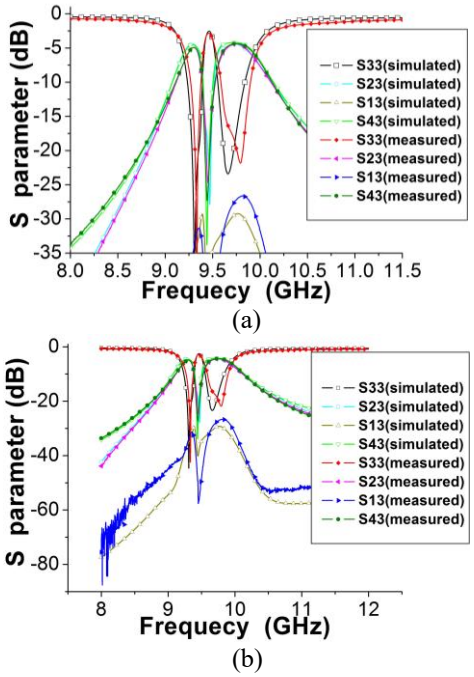

Fig. 13. Simulated and measured results of the fabricated dual-band filtering coupler: (a) and (b) Port 3 is excited.

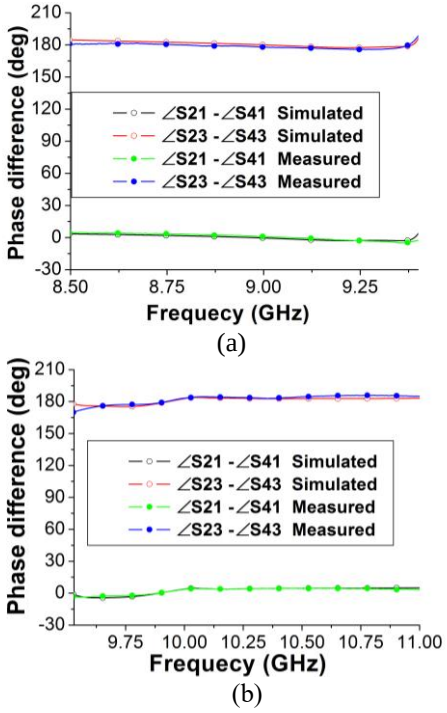

Fig. 14. Phase differences of the fabricated multilayer dual-band filtering coupler: (a) first passband and (b) second passband.

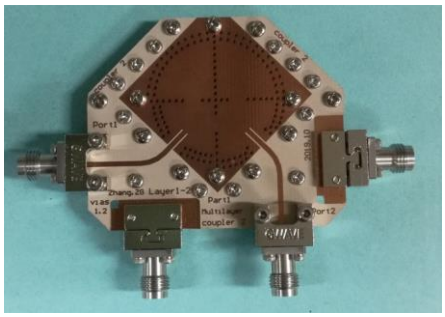

Fig. 15. Photograph of the fabricated multilayer dual-band filtering rat-race coupler.

Figure 15 is the photograph of the fabricated multilayer dual-band filtering rat-race coupler.

A detailed performance comparison with filtering couplers in recent years is shown in Table 1. Compared with [16] and [17], the proposed design has much higher Q factor and self-consistent electromagnetic shielding structure, which is suitable for higher frequency operation. In [19], although the Q factor of the filtering coupler is very high, the 3-D DR structure with large height makes it more difficult to be integrated with other planar circuits. A single-band filtering rat-race coupler based on the orthogonal modes is proposed in [25]. The desired 0° and 180° phase differences are realized by the inherent characteristics of TE_{102} and TE_{201} modes. Therefore, the input port and isolation port, as well as the two output ports, must be kept perpendicular to each other, which makes the phase characteristics and isolation dependent on the port direction. In [26], a novel coupler with arbitrary division, optional phase difference, and alternative input/output impedances is presented for the first time. Based on hybrid couplers, a microwave device able to detect differential-mode to common-mode conversion is proposed in [27]. A dual-mode hybrid coupler, capable of providing distinguished functions as rat-race couplers at two frequency bands, is first demonstrated in [28]. Compared with the works in [16-28], the proposed structure not only has relatively high Q factor, better isolation, flexibly controlled bandwidth ratio, simple structure, but also can be suitable for the application of multiple operation band, which is helpful to achieve high density and miniaturized RF/microwave wave system.

Table 1: Performance comparison of various filtering rat-race couplers

Ref.	f_0 (GHz)/ FBW (%)/ε_r	IL (dB)/ Isolation (dB)/Q factor	Mag.(dB)/ Phase (deg) Imbalance	AOB*	Circuit Size	Techniques/ Layers*
[16]	2.4/10/2.2	0.7/20/80	1/2	1	$0.32\times0.32\lambda_g^2$	Microstrip/1
[17]	0.47/13/3.38	1.17/25/60	0.2/4.5	1	$0.23\times0.12\lambda_g^2$	Microstrip/1
[19]	1.94/0.5/38	1.2/23/2000	0.3/5	1	$0.29\times0.29\lambda_g^2$	DR/-
[22]	20/2.6/2.2	1.63/28/190	0.3/5	1	$2.51\times2.51\lambda_g^2$	SIW/1
[23]	11/3.6/3.5	1.6/20/170	0.6/8	1	$1.59\times1.26\lambda_g^2$	SIW/1
[24]	7.75/2.7/3.5	1.5/25/200	0.6/5	1	$0.79\times0.45\lambda_g^2$	SIW/2
[25]	11.8/3.5/3.5	1.3/18/210	0.1/3	1	$1.18\times1.18\lambda_g^2$	SIW/1
This work	9.30,9.73/1.6,3.1/3.5	1.92,1.35/30,27/210	0.05/3	2 dual-band	$1.19\times1.19\lambda_g^2$	SIW/2

Where λ_g is the guided wavelength on the substrate at the center frequency f_0, FBW represents the fractional bandwidth. **AOB*** represents the number of available operation bands. Layers* represents the number of substrate layers.

IV. CONCLUSION

In this paper, a compact multilayer dual-band filtering rat-race coupler based on substrate integrated fan-shaped cavities (SIFCs) is proposed for the first time. Simulated and measured results have been presented to verify the proposed method. Magnetic and electric coupling between SIFCs are realized through multiple rectangular slots and circular slots etched on metal layer, respectively. What's unique about the analysis process of dual-band filtering rat-race coupler is that the bandwidth and center frequency of the corresponding broadband coupler can be obtained from the specification of dual-band filtering coupler. The required coupling coefficient and external quality factor can be obtained by analyzing the topology of the single-band filtering coupler. Afterwards, the coupling matrix method is used to evaluate the initial value of design parameters accurately according to the specifications. Generally, the proposed designs have shown excellent performance of dual-band filtering responses, isolation, amplitude balance, 0° and 180° phase differences, as well as the compact structure. The proposed multilayer SIFCs dual-band filtering rat-race coupler could be more suitable for the development of high density and miniaturized RF/microwave system.

ACKNOWLEDGMENT

This work was supported in part by the Ministry of Science and Technology of the People's Republic of China under grant 2013YQ200503 and in part by the National Natural Science Foundation of China (NSFC)

under grant 61001028.

REFERENCES

[1] X.-P. Chen, K. Wu, and Z.-L. Li, "Dual-band and triple-band substrate integrated waveguide filters with Chebyshev and quasi-elliptic responses," *IEEE Trans. Microw. Theory Techn*., vol. 55, no. 12, pp. 2569-2578, Dec. 2007.

[2] Y. Dong and T. Itoh, "Miniaturized dual-band substrate integrated waveguide filters using complementary split-ring resonators," *IEEE MTT-S Int. Microw. Symp. Dig*., pp. 1-4, June 2011.

[3] K. Song and Q. Xue, "Novel ultra-wideband (UWB) multilayer slotline power divider with bandpass response," *IEEE Microw. Wirel. Compon. Lett*., vol. 20, no. 1, pp. 13-15, Jan. 2010.

[4] Y. J. Cheng, W. Hong, and K. Wu, "94 GHz substrate integrated monopulse antenna array," *IEEE Trans. Antennas Propag*., vol. 60, no. 1, pp. 121-128, Jan. 2012.

[5] Y. J. Cheng, W. Hong, K. Wu, and Y. Fan, "A hybrid guided-wave structure of half mode substrate integrated waveguide and conductor-backed slotline and its application in directional couplers," *IEEE Microw Wireless Compon Lett*., vol. 21, no. 2, pp. 65-67, Feb. 2011.

[6] Z.-G. Zhang, Y. Fan, Y. J. Cheng, and Y.-H. Zhang, "A compact multilayer dual-mode substrate integrated circular cavity (SICC) filter for X-band application," *Prog. Electromagn. Res*., vol. 122, no. 1, pp. 453-465, Jan. 2012.

[7] H. Zhang, W. Kang, and W. Wu, "Miniaturized dual-band SIW filters using E-shaped slotlines with controllable center frequencies," *IEEE Microw. Wireless Compon. Lett*., vol. 28, no. 4, pp. 311-313, Apr. 2018.

[8] Z.-G. Zhang, Y. Fan, and Y.-H. Zhang, "Compact 3-D multilayer substrate integrated circular and elliptic cavities (SICCs and SIECs) dual-mode filter with high selectivity," *Appl. Comp. Electro. Society (ACES) Journal*, vol. 28, no. 4, pp. 333-340, Apr. 2013.

[9] Q. Chen and J. Xu, "Out-of-phase power divider based on two-layer SIW," *Electron Lett*., vol. 50, no. 14, pp. 1005-1007, July 2014.

[10] X. Guo, L. Zhu and W. Wu, "Design method for multiband filters with compact configuration in substrate integrated waveguide," *IEEE Trans. Microw. Theory Tech*., vol. 66, no. 6, pp. 3011-3018, June 2018.

[11] P.-L. Chi and T.-Y. Chen, "Dual-band ring coupler based on the composite right/left-handed folded substrate-integrated waveguide," *IEEE Microw. Wireless Compon. Lett*., vol. 24, no. 5, pp. 330-332, May 2014.

[12] Y. J. Wang, C.-X. Zhou, K. Zhou, and W. Wu, "Compact dual-band filtering power divider based on SIW triangular cavities," *Electron Lett*., vol. 54, no.18, pp. 1072-1074, Sep. 2018.

[13] H. Uchida, N. Yoneda, and S. Makino, "Bandpass directional couplers with electromagnetically-coupled resonators," *IEEE MTT-S Int. Microwave Symp. Digest*., pp. 1563-1566, June 2006.

[14] L.-S. Wu, B. Xia, W.-Y. Yin, and J. Mao, "Collaborative design of a new dual-bandpass 180° hybrid coupler," *IEEE Trans. Microw. Theory Tech*., vol. 61, no. 3, pp. 1053-1066, Mar. 2013.

[15] P. Li, H. Chu, and R.S. Chen, "SIW magic-T with bandpass response," *Electron Lett*., vol. 51, no. 14, pp. 1078-1080, July 2015.

[16] C.-K. Lin and S.-J. Chung, "A compact filtering 180° hybrid," *IEEE Trans. Microw. Theory Tech*., vol. 59, no. 12, pp. 3030-3036, Dec. 2011.

[17] K.-X. Wang, X.-Y. Zhang, S.-Y. Zheng, and Q. Xue, "Compact filtering rat-race hybrid with wide stopband," *IEEE Trans. Microw. Theory Tech*., vol. 63, no. 8, pp. 2250-2560, Aug. 2015.

[18] J.-X. Xu, X.-Y. Zhang, and H.-Y. Li, "Compact narrowband filtering rat-race coupler using quad-mode dielectric resonator," *IEEE Trans. Microw. Theory Tech*., vol. 66, no. 9, pp. 4029-4039, Sep. 2018.

[19] L.-X. Jiao, Y.-L. Wu, Y.-N. Liu, W.-M. Wang, and J.-X. Chen, "Concept for narrow-band filtering rat-race coupler using dual-mode cross-shaped dielectric," *Electron Lett*., vol. 52, no. 3, pp. 212-213, Feb. 2016.

[20] K.-X. Wang, X.-F. Liu, Y.-C. Li, L.-Z. Lin, and X.-L. Zhao, "LTCC filtering rat-race coupler based on eight-line spatially-symmetrical coupled structure," *IEEE Access*, vol. 6, no. 6, pp. 262-269, June 2018.

[21] Z.-G. Zhang, Y. Fan, and Y.-H. Zhang, "Multilayer half-Mode substrate integrated waveguide wide-band coupler with high selectivity," *Appl. Comp. Electro. Society (ACES) Journal*, vol. 34, no. 9, pp. 1418-1425, Sep. 2019.

[22] S.-Q. Han, K. Zhou, J.-D. Zhang, C.-X. Zhou, and W. Wu, "Novel substrate integrated waveguide filtering crossover using orthogonal degenerate modes," *IEEE Microw. Wireless Compon. Lett*., vol. 27, no. 9, pp. 803-805, Sep. 2017.

[23] U. Rosenberg, M. Salehi, J. Bornemann, and E. Mehrshahi, "A novel frequency-selective power combiner/divider in single-Layer substrate integrated waveguide technology," *IEEE Microw. Wireless Compon. Lett*., vol. 23, no. 8, pp. 406-408, Aug. 2013.

[24] Y.-J. Cheng and Y. Fan, "Compact substrate-integrated waveguide bandpass rat-race coupler and its microwave applications," *IET Microw., Antennas Propag*., vol. 6, no. 9, pp. 1000-1006, June 2012.

[25] H.-Y. Li, J.-X. Xu, and X.-Y. Zhang, "Substrate

integrated waveguide filtering rat-race Coupler based on orthogonal degenerate modes," *IEEE Trans. Microw. Theory Techn*., vol. 67, no. 1, pp. 140-150, Jan. 2019.

[26] Y. L. Wu, L. X. Jiao, Q. Xue, and Y. A. Liu, "A universal approach for designing an unequal branch-line coupler with arbitrary phase differences and input/output impedances," *IEEE Trans. Compon., Packag., Manuf. Technol*., vol. 7, no. 6, pp. 944-955, June 2017.

[27] J. Muñoz-E., P. Vélez, M. G. Barba, J. Mata-C., and F. Martín, "Differential-mode to common-mode conversion detector based on rat-race hybrid couplers: analysis and application to differential sensors and comparators," *IEEE Trans. Microw. Theory Tech*., vol. 68, no. 6, pp. 1-14, June 2020.

[28] H. N. Chu, G.-Y. Li, and T.-G. Ma, "Dual-mode coupler with branch-line/rat-race responses on integrated passive device process," *IEEE MTT-S Int. Microw. Workshop Series on Advanced Materials and Processes. RF, THz. Appl. (IMWS-AMP)*, Bochum, Germany, pp. 82-84, Oct. 2019.

[29] M.-K. Li, C. Chen, and W. Chen, "Miniaturized dual-band filter using dual-capacitively loaded SIW cavities," *IEEE Microw. Wireless Compon. Lett*., vol. 27, no. 4, pp. 344-346, Apr. 2017.

[30] S. Zhang, J.-Y. Rao, J.-S. Hong, and F.-L. Liu, "A novel dual-band controllable bandpass filter based on fan-shaped substrate integrated waveguide," *IEEE Microw. Wireless Compon. Lett*., vol. 28, no. 4, pp. 308-310, Apr. 2018.

[31] Y.-D. Dong and T. Itoh, "Miniaturized substrate integrated waveguide slot antennas based on negative order resonance," *IEEE Trans. Antennas Propag*., vol. 58, no. 12, pp. 3856-3864, Dec. 2010.

[32] J.-S. Hong and M.-J. Lancaster, *Microstrip Filter for RF/Microwave Applications*. New York, NY, USA: Wiley, 2001.

[33] R.-J. Cameron, "Advanced coupling matrix synthesis techniques for microwave filters," *IEEE Trans. Microw. Theory Tech*., vol. 51, no. 1, pp. 1-10, Jan. 2003.

[34] D.-M. Pozar, *Microwave Engineering*, second edition, New York: Wiley, 1998.

Zhigang Zhang was born in Shanxi Province, China. He received the B.S. degree in Electronic Information Engineering and M.S. degree in Wireless Physics from Sichuan University and is currently working toward the Ph.D. degree in Electromagnetic Field and Microwave Technology from The University of Electronic Science and Technology of China (UESTC), Chengdu, Sichuan, China. His current research interests include SIW technology and its application, microwave and millimeter-wave filters and couplers, electromagnetic theory.

Yong Fan received the B.E. degree from the Nanjing University of Science and Technology, Nanjing, Jiangsu, China, in 1985, and the M.S. degree from the University of Electronic Science and Technology of China (UESTC), Chengdu, Sichuan, China, in 1992.

He is currently with the School of Electronic Engineering, UESTC. He has authored or coauthored over 60 papers. From 1985 to 1989, he was interested in microwave integrated circuits. Since 1989, his research interests include millimeter-wave communication, electromagnetic theory, millimeter-wave technology, and millimeter-wave systems. Mr. Fan is a Senior Member of the Chinese Institute of Electronics (CIE).

Yujian Cheng was born in Sichuan, China, in 1983. He received the B.S. degree from University of Electronic Science and Technology of China, in 2005 and the Ph.D. degree from Southeast University, Nanjing, China, in 2010. Since 2010, he has been with University of Electronic Science and Technology of China, and is currently a Professor. His current research interests include microwave and millimeter-wave antennas, arrays and circuits. He has authored or coauthored more than 100 articles in journals and conferences, as well as a book—Substrate Integrated Antennas and Arrays, (CRC Press, 2015). Cheng was the recipient of the National Science Fund for Excellent Young Scholars in 2016, Chang Jiang Scholars Program (Young Scholars) in 2016, and National Excellent Doctorate Dissertation of China in 2012. Now, Cheng serves as an Associate Editor for IEEE Antennas and Propagation Letters

Yonghong Zhang received the B.S., M.S., and Ph.D. degrees from the University of Electronic Science and Technology of China (UESTC), Chengdu, China, in 1992, 1995, and 2001, respectively. From 1995 to 2002, he was a Teacher with the UESTC. In 2002, he joined the Electronic Engineering Department, Tsinghua University, Beijing, China, as a Doctoral Fellow. In 2004, he rejoined the UESTC. His research interests are in the area of microwave and millimeter-wave technology and applications.